LOW-RANK MATRIX COMPLETION FOR DISTRIBUTED AMBIENT NOISE IMAGING SYSTEMS

Danye Xu[⋆] *Bingqing Song*[⋆] *Yao Xie*[†] *Sin-Mei Wu*[‡] *Fan-Chi Lin*[‡] *WenZhan Song*[•]

[⋆] University of Science and Technology of China, Hefei, Anhui, China.
[†]School of Industrial and Systems Engineering, Georgia Institute of Technology, Atlanta, GA, USA.
[‡]Dept. of Geology and Geophysics, University of Utah, Salt Lake City, UT, USA.
[•]College of Engineering, University of Georgia, Athens, GA, USA.

ABSTRACT

We present a new approach to address the "missing data" issue in the distributed ambient noise imaging (ANSI) system, a promising new seismic imaging paradigm for shallow earth surfaces. Missing data is inevitable in distributed ANSI: due to communication constraint and weak signals, not all pairs of cross-correlation functions between sensors contain useful information (i.e., a significant peak). Without completing the missing data, we cannot use the conventional ambient noise imaging methods, which requires to know the complete pairs of cross-correlation between sensors. We show that the problem can be formulated as a low-rank matrix completion problem, and leverage the recent advances in this field to present an efficient algorithm. Simulated and real-data examples demonstrate the promising performance of our approach. [1]

1. INTRODUCTION

ANSI (Ambient Noise Imaging) is a promising new paradigm for seismic imaging. ANSI makes use of *ambient noises* recorded by sensors. The most crucial step in imaging is to compute pairwise cross-correlation functions between sensors, and finding the location of "peak" of the cross-correlation functions, which is used in the subsequent frequency-time analysis to form images [1]. Compared with conventional active imaging, which usually requires strong sources that are artificially introduced (such as dynamite explosion), ANSI uses natural sources of "signals", which is non-invasive and more environmentally friendly. The ANSI is particularly useful for imaging shallow earth structures.

In the recently developed distributed ANSI systems [2] for real-time imaging, sensors perform pairwise cross-correlation in real-time using continuous data streams. Due to communication and computation constraint, we may not be able to require all sensors to communicate with each other (to form $N(N-1)/2$ cross-correlation function, where N is the number of sensors). Each sensor is only able to communicate with their neighboring sensors. On the other hand, in practice, there will be pairs of sensors where "signal" is missing, i.e., when performing cross-correlation between these pairs, there is no significant "peak" in the cross-correlation, which indicates somehow the signal might be missing (due to sensor measurement errors, or the signal-to-noise ratio is too weak). Due to the two above reasons, we are not able to obtain cross-correlation functions between all pairs of sensors. However, the conventional ambient noise imaging algorithms require cross-correlation between all pairs of sensors. Therefore, we need to complete the missing information: the information between the pairs of sensors that we are not able to find cross-correlation.

In this paper, we address the missing data problem in distributed ANSI, using rank-one matrix completion. In particular, we show that the problem has a rank-one structure (which could be explained by the fact that usually there is one strong dominating signal source). This allows us to leverage the recent advances in low-rank matrix completion (see, e.g., [3, 4]) to solve this problem efficiently. We demonstrate the promising performance of our approach using simulated examples and a real-data set measured at Yellowstone Old Faithful geyser.

On a high level, the problem we are facing in ANSI is related to the delay estimation. However, our problem differs from the array signal processing (for instance, the well-known MUSIC algorithm [5]), since we do not have a uniform linear array as considered in these classic works. Our problem is also different from the localization using delay estimate (e.g., [6]) since we cannot measure the relative delay directly. Our problem can be viewed as a special case of signal synchronization [7], however, here we focus specially on missing data aspect of the problem.

2. FORMULATION

Assume there are N sensors. In ANSI, usually it is assumed there is one unknown dominant ambient noise "source", which we represent using $s(t)$. Each sensor observes a con-

[1]The first two authors contribute equally. The work was done during their visit to Georgia Institute of Technology. The work is sponsored by NSF CCF-1442635.

taminated and delayed version of the source signal:

$$x_n(t) = \rho_n s(t - \tau_n) + \eta_n(t), t = 0, \ldots, T-1, \forall n \quad (1)$$

where T is the number of samples, and $\eta_n(t)$ is Gaussian noise.

In ANSI, the ambient noise source is usually very weak, so we can only detect the signal by performing cross-correlation two long recorded sequences (T is usually large). We are interested in estimating the pairwise delays between sensors:

$$\Delta_{nm} = \tau_n - \tau_m,$$

using cross-correlation function. The (zero-padded) cross-correlation between a pair of sensors indexed by n and m is given by

$$r_{nm}(t) = x_n(t) \star x_m(t) \triangleq \sum_{\ell} x_n(\ell) x_m(t+\ell).$$

where $\star$ denotes convolution. Note that due to communication constraint and missing data, we are only able to observe a subset of cross-correlation functions in $\Omega \subset [1, \ldots, N] \times [1, \ldots, N]$, i.e., we only know r_{nm} for $(n, m) \in \Omega$. Our goal is to complete Δ_{nm}, based on observations of $r_{nm}(t)$ on $(n, m) \in \Omega$.

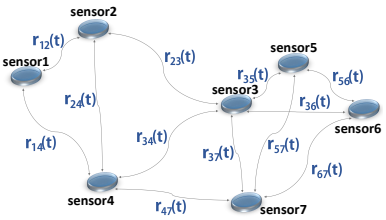

Fig. 1. Problem setup for ambient noise imaging, where $r_{nm}(t)$ denotes pairwise cross-correlation functions, and we can only observe $(n, m) \in \Omega$.

3. RANK-ONE MATRIX COMPLETION

First we show the rank-one structure of the problem. Define the discrete Fourier transform of signals

$$X_n(k) = \sum_{\ell} x_n(\ell) e^{-i2\pi f_k}, k = 0, 1, \cdots, T-1, \forall n,$$

where $f_k \triangleq 2\pi k/T$, and $i = \sqrt{-1}$. In the frequency domain, cross-correlation becomes multiplication:

$$\begin{aligned} R_{nm}(k) &= X_n^*(k) X_m(k) \\ &= |S(k)|^2 e^{i f_k \Delta_{nm}} + N_{nm}(k), k = 0, 1, \cdots, T-1. \end{aligned} \quad (2)$$

where $*$ denotes the conjugate operation, and $N_{nm}(k)$ denotes noise terms, which may also depend on signal. Define matrices $\mathbf{R}(k) \in \mathbb{C}^{N \times N}$, $k = 0, 1, 2, \cdots, T-1$, whose entry is given by $\mathbf{R}_{nm}(k)$. Also define

$$\mathbf{h}_k = (e^{-\tau_1 f_k}, e^{-\tau_2 f_k}, \cdots, e^{-\tau_N f_k})^T.$$

From (2), we can show that these matrices are rank-one:

$$\mathbf{R}(k) = |S(k)|^2 \mathbf{h}_k \mathbf{h}_k^H + \mathbf{N}(k), k = 0, 1, \cdots, T-1,$$

Define the phase angle of a complex number to be θ, and consider the phase angle of each $\mathbf{R}(k) \in \mathbb{C}^{N \times N}$, $k = 0, 1, 2, \cdots, T-1$, the formula gives an estimation of the lag time $\Delta_{nm} = \theta(\mathbf{R}(k))T/2\pi k$. We construct a matrix $\mathbf{R}(k)$, in which each entry $\mathbf{R}_{nm}(k)$ stands for the lag time between the two sensors in a pair. We can show the matrix is rank-1:

$$\mathbf{R}(k) = |S(k)|^2 \mathbf{h}_k \mathbf{h}_k^H + \mathbf{N}(k), k = 0, 1, \cdots, T-1, \quad (3)$$

where $\mathbf{N}(k)$ is noise, $\mathbf{h}_k^H$ refers to the Hermitian of $\mathbf{h}_k$, and the vector $\mathbf{h}_k = (e^{-\tau_1 f_k}, e^{-\tau_2 f_k}, \cdots, e^{-\tau_N f_k})^T$.

3.1. Low-rank matrix completion

Now formulation (3) will enable us to use low-rank matrix completion (LRMC) to infer the missing entries. The completed matrix can be solved using the following nuclear minimization problem (for each k)

$$\begin{array}{ll} \min\limits_{X} & \|\mathbf{X}\|_* \\ \text{subject to} & \sum_{(i,j)\in\Omega} (X_{ij} - R_{ij}(k))^2 \leqslant \delta, \end{array} \quad (4)$$

where $\|\mathbf{X}\|_*$ denote the nuclear norm of $\mathbf{X}$, $\delta \geq 0$ is the tolerance parameter [8]. We need to solve $N-1$ LRMC problems. There are various efficient algorithms to solve the matrix completion problem (e.g., iterative singular value thresholding [9], using non-convex formulation and alternating minimization [10].)

3.2. Delay estimate based on completed matrices

Finally we relate the recovered matrices to relative delay estimates. After solving K matrix completion problems, we obtain solutions $\hat{\mathbf{R}}(k)$. We can extract the leading eigenvector for each solution, which can be treated as an estimate for $\mathbf{h}_k$. Let $\theta(z)$ denote the phase angle of a complex number z. Thus, we have that

$$\theta([\hat{\mathbf{R}}(\mathbf{k})]_{nm}) \approx \frac{2\pi \Delta_{nm} k}{N}, \quad k = 1, \ldots, K, \quad \forall n, m.$$

Then for each (n, m), we have K equations for Δ_{nm}. We use least square to estimate Δ_{nm}, i.e., fitting a line to relate K points: $(k, \theta([\hat{\mathbf{R}}(\mathbf{k})]_{nm}))$, and the slope of the line will be an estimate for $2\pi\Delta_{nm}/N$.

3.3. Maximal-likelihood delay estimation

We can also derive the maximum likelihood estimate (MLE) for the delay, for each pair of sensors that we have data to compute cross-correlation function (the derivation of MLE can be found in appendix). MLE, being an asymptotic efficient estimator, may serve as a bench mark for the accuracy of our low-rank matrix completion algorithm (as we show in numerical example section). Assume the noise in observation (1) is Gaussian with zero mean and variance σ^2. Denote $\hat{S}(k)$

as the MLE of the signal. Using the definition of the cross-correlation function (2), it can be shown that the following quantity is approximately χ^2 distributed with two degree-of-freedom (denote its probability distribution function as f):

$$G_k(\tau) = (X_n(k) - \hat{S}(k)e^{-\tau f})^*(X_m(k) - \hat{S}(k)).$$

We can estimate Δ_{nm} by

$$\hat{\tau} = \arg\max_{\tau} \sum_{k=0}^{T-1} \log f\left(\frac{|G_k(\tau)|}{\sigma_0}\right),$$

where $f(x) = x^{-\frac{1}{2}}e^{-\frac{x}{2}}/(\sqrt{2}\gamma(\frac{1}{2}))$, which is the density function of a χ^2 variable with two.

4. NUMERICAL EXAMPLES

In this section, we verified the accuracy of our proposed method using simulation and real-data.

4.1. Simulation

The influence of noise variance on the error between the true lag time and the lag time predicted by our method is studied in the following simulations. We adopt the usual performance metric RMSE $= (1/N)\sum_{i=1}^{N}(\tau_{\text{predicted,i}} - \tau_{\text{true,i}})^2)^{1/2}$.

Comparison with MLE. First, we compare the accuracy of the estimates obtained by rank-one matrix completion and that by MLE. We show that the proposed approach can obtain good accuracy that is close to MLE, but remember that our approach is computationally much more efficient. We generate $N = 9$ sensors, with random positive delays τ_i. The source s is a Gaussian-shaped signal. The results show that the larger the variance of the noise between each pair of signals, the larger the error between lag time predicted using our method and the real lag time we set. What's more, the RMSE of MLE is only a little bit smaller than our method, which means our method is accurate and easy enough. And the reason why we do not use MLE on real data is that MLE is based on an exact distribution of noises, while the practical noises of real signals is unknown.

RMSE with randomly missing data. We generate instances with randomly missed entries. The results are shown in ..., which show the MSE for relative delay estimate for three pairs of sensors (denoted by Δ_1, Δ_2, and Δ_3).

RMSE with missing data due to distance. In this section, we simulated a scenario, where sensors are arbitrarily places in three dimensional spaces. We assume sensors that are more far apart, with distance greater than certain threshold, whose cross-correlation functions are missing. This is to mimic the situation in distributed ANSI, the sensors are only able to communicate with their neighbors, since signals are transmitted wirelessly and the channels between far away sensors is usually not available due to path loss and mutual interference. Note that the MSE of the estimated delay are quite reasonable.

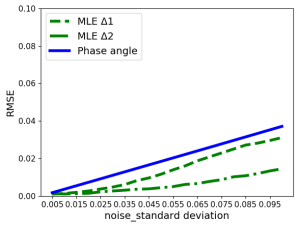

(a) Comparison with MLE

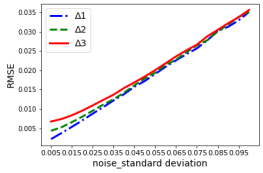

(b) random missing

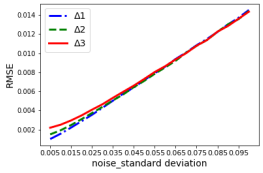

(c) missing due to long distance

Fig. 2. The lines with different Δ indicate different lag times between signals, and $\Delta_1 < \Delta_2 < \Delta_3$. The y axis is the RMSE between the lag time we predicted and the real lag time we set to each signal. And the noise_standard deviation means the standard deviation of noise we add to signals.

4.2. Real-data

In this section, we use a real dataset to demonstrate the good performance of our method. From 2015/11/06 on and for a week, 16 geophone sensors are placed around Old Faithful Geyser in Yellowstone National Park to record signal continuously (the sampling frequency is 500 Hz). Sensors are indexed 001, 002, ... 016 below. The locations of the sensors are shown in Fig. 3. First, we perform cross-correlation between pairs of sensors. When performing cross-correlation, we truncated the signal into 5-minute segments, and there are 120 segments. We perform cross-correlation for the 5 minute segments, and average the cross-correlation functions over all segments (for each pair of sensors). The averaging is shown to be essential in boosting the signal. Then we band-pass filtering the results in 1-5 Hz (which, according to geophysicts' experience, contain interesting information which is likely to be related to Old Faithful Geyser's activity [11]).

Signal detection. As a first step, we have to decide whether there is a "peak" between a pair of sensors. We did this by computing the cross-correlation functions between all pairs of sensors. We then examine the peaks of the cross-correlation functions, and find out the maximum peak values across all cross-correlation functions. Then we set a threshold, which is 7% of the maximum peak value. We decide all pairs whose peak values are below the threshold to be the ones that does not contain a "peak", i.e., the signal is missing. This create a missing pattern, as shown in the block holes in Fig. 4(a). The cross-correlation functions for all sensors are shown in appendix. We also find that sensor 007 does not contain any

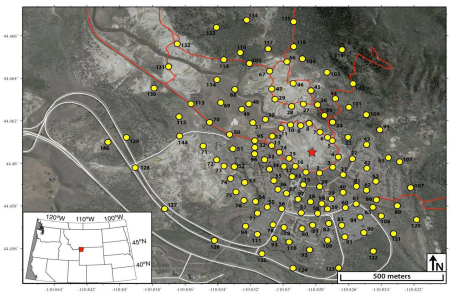

Fig. 3. Sensor deployment in Yellowstone National Park to collect ambient noise signals. There are total of 135 sensors (labeled in picture) and we only used the first 16 sensors in our study as a proof of concept.

signal in any of its cross-correlation functions, so we removed it from study. This gives $N = 15$ sensors and a 15-by-15 matrix to complete.

Verify rank-one assumption. Now we form the $\mathbf{R}(k)$ matrices using frequency samples of the cross-correlation functions. We verify the rank-one property of these matrices as follows. We will out the missing entries by zero, and compute the singular value decomposition (in this case, the eigen-decomposition also works since the matrix is Hermitian). The eigenvalues of $\hat{\mathbf{R}}(k)$ are real, since the matrices are all Hermitian. The eigenvalues for $\hat{\mathbf{R}}(1)$ is shown in Fig. 4, which clearly shows that the matrix is nearly rank-one. The situation for all the other matrices are similar. This means that we can indeed use our approach to infer the missing entries.

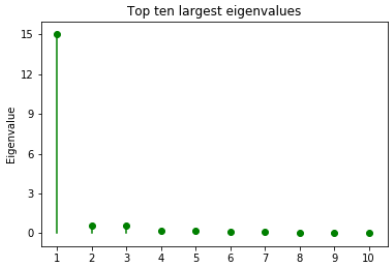

Fig. 4. Top 10 eigenvalues of zero-filled $\hat{\mathbf{R}}(1)$. This shows that our rank-one assumption holds.

Accuracy. Now we study the accuracy of our approach. Since there is no ground truth in our study, we use the following method. Fig. 6(a) shows the relative delay matrices, between all 15 sensors (the value of the matrix is the relative delay). Note that the matrix is per-symmetric. The blue entries are missing, whose values are recovered using our method. Now we cover up some randomly chosen entries, pretending their cross-correlation functions are missing, using our method to recover their values and compare with the observed values (i.e., in Fig. 6(a)). Fig. 6(b) shows the matrix obtained this way, where the green entries are the "covered-up" ones. Note that indeed, the green entries matches pretty well with their correspondence in Fig. 6(a).

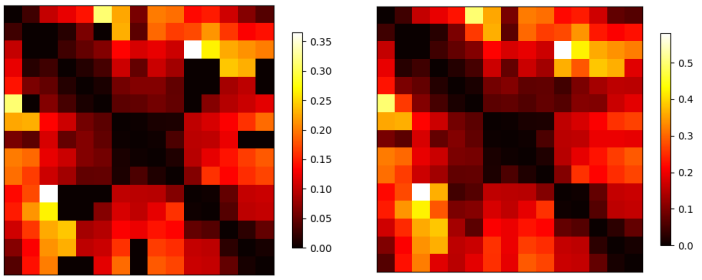

(a) (b)

Fig. 5. Heat map of the relative delay matrix Δ_{nm}: (a) the missing entries correspond to black holes; (b) recovered matrix using our method.

sensors	0 0 1	0 0 2	0 0 3	0 0 4	0 0 5	0 0 6	0 0 8	0 0 9	0 1 0	0 1 1	0 1 2	0 1 3	0 1 4	0 1 5	0 1 6
0 0 1	0	-0.046	-0.163	0.194	0.229	0.499	0.357	0.097	0.319	0.309	0.220	0.236	0.171	0.109	0.064
0 0 2	0.046	0	-0.001	0.027	0.100	0.282	0.364	0.073	0.302	0.266	0.277	0.341	0.261	0.211	0.227
0 0 3	0.163	0.001	0	0.047	0.079	0.107	0.214	0.179	0.194	0.168	0.582	0.423	0.361	0.340	0.321
0 0 4	-0.194	-0.027	-0.047	0	0.023	0.054	0.169	0.077	0.167	0.134	0.441	0.347	0.386	0.364	0.244
0 0 5	-0.229	-0.010	-0.079	-0.023	0	0.015	0.093	0.105	0.105	0.075	-0.067	-0.099	-0.136	-0.157	-0.176
0 0 6	-0.499	-0.282	-0.107	-0.054	-0.015	0	0.071	0.077	0.093	0.079	-0.108	-0.108	-0.150	-0.167	-0.189
0 0 8	-0.357	-0.364	-0.214	-0.169	-0.093	-0.071	0	0.003	0.014	0.017	-0.159	-0.178	-0.210	-0.256	-0.306
0 0 9	-0.097	-0.073	-0.179	-0.077	-0.105	-0.077	-0.003	0	-0.005	0.059	-0.153	-0.157	-0.197	-0.237	-0.235
0 1 0	-0.319	-0.302	-0.194	-0.167	-0.105	-0.093	-0.014	0.005	0	0.020	-0.152	-0.193	-0.229	-0.265	-0.289
0 1 1	-0.309	-0.266	-0.168	-0.134	-0.075	-0.079	-0.017	-0.059	-0.020	0	-0.106	-0.256	-0.215	-0.250	-0.271
0 1 2	-0.220	-0.277	-0.582	-0.441	0.067	0.108	0.159	0.153	0.152	0.106	0	-0.006	-0.078	-0.162	-0.167
0 1 3	-0.236	-0.341	-0.423	-0.347	0.099	0.108	0.178	0.157	0.193	0.256	0.006	0	-0.065	-0.156	-0.161
0 1 4	-0.171	-0.261	-0.361	-0.386	0.136	0.150	0.210	0.197	0.229	0.215	0.078	0.065	0	-0.032	-0.078
0 1 5	-0.109	-0.211	-0.340	-0.364	0.157	0.167	0.256	0.237	0.265	0.250	0.162	0.156	0.032	0	-0.013
0 1 6	-0.064	-0.227	-0.321	-0.244	0.176	0.189	0.306	0.235	0.289	0.271	0.167	0.161	0.078	0.013	0

(a)

sensors	0 0 1	0 0 2	0 0 3	0 0 4	0 0 5	0 0 6	0 0 8	0 0 9	0 1 0	0 1 1	0 1 2	0 1 3	0 1 4	0 1 5	0 1 6
0 0 1	0	-0.046	-0.163	0.194	0.229	0.499	0.357	0.097	0.319	0.309	0.220	0.236	0.171	0.090	0.064
0 0 2	0.046	0	-0.001	0.027	0.100	0.282	0.364	0.073	0.302	0.266	0.277	0.341	0.241	0.211	0.227
0 0 3	0.163	0.001	0	0.047	0.079	0.107	0.214	0.179	0.194	0.168	0.582	0.423	0.361	0.340	0.321
0 0 4	-0.194	-0.027	-0.047	0	0.023	0.054	0.169	0.077	0.167	0.134	0.441	0.347	0.386	0.364	0.244
0 0 5	-0.229	-0.010	-0.079	-0.023	0	0.015	0.093	0.105	0.087	0.075	-0.067	-0.099	-0.136	-0.157	-0.176
0 0 6	-0.499	-0.282	-0.107	-0.054	-0.015	0	0.071	0.077	0.078	0.079	-0.108	-0.108	-0.089	-0.167	-0.189
0 0 8	-0.357	-0.364	-0.214	-0.169	-0.093	-0.071	0	0.003	0.014	0.017	-0.159	-0.178	-0.210	-0.256	-0.262
0 0 9	-0.097	-0.073	-0.179	-0.077	-0.105	-0.077	-0.003	0	-0.005	0.059	-0.153	-0.157	-0.197	-0.237	-0.235
0 1 0	-0.319	-0.302	-0.194	-0.167	-0.087	-0.078	-0.014	0.005	0	0.020	-0.152	-0.193	-0.229	-0.265	-0.289
0 1 1	-0.309	-0.266	-0.168	-0.134	-0.075	-0.079	-0.017	-0.059	-0.020	0	-0.106	-0.256	-0.215	-0.250	-0.271
0 1 2	-0.220	-0.277	-0.582	-0.441	0.067	0.108	0.159	0.153	0.152	0.106	0	-0.006	-0.078	-0.162	-0.167
0 1 3	-0.236	-0.341	-0.423	-0.347	0.099	0.108	0.178	0.157	0.193	0.256	0.006	0	-0.065	-0.156	-0.161
0 1 4	-0.171	-0.241	-0.361	-0.386	0.136	0.089	0.210	0.197	0.229	0.215	0.078	0.065	0	-0.032	-0.078
0 1 5	-0.090	-0.211	-0.340	-0.364	0.157	0.167	0.256	0.237	0.265	0.250	0.162	0.156	0.032	0	-0.013
0 1 6	-0.064	-0.227	-0.321	-0.244	0.176	0.189	0.262	0.235	0.289	0.271	0.167	0.161	0.078	0.013	0

(b)

Fig. 6. a) Relative delay matrix: blue entries are filled by matrix completion; (b) Relative delay matrix: green entries.

5. CONCLUSION

In this paper, we present a low-rank matrix completion based approach, for the missing data issue in the distributed ambient noise imaging systems. Simulated and real-data examples demonstrate the good performance of our approach. (The appendix can be found at www2.isye.gatech.edu/∼yxie77/ICASSP2019-appendix.pdf)

6. REFERENCES

[1] Fan-Chi Lin, Morgan P. Moschetti, and Michael H. Ritzwoller, "Surface wave tomography of the western united states from ambient seismic noise: Rayleigh and Love wave phase velocity maps," *Geophys. J. Int.*, 2008.

[2] M. Valero, J. Clemente, G. Kamath, Y. Xie, F.-C. Lin, and W. Song, "Real-time ambient noise subsurface imaging in distributed sensor networks," in *IEEE International Conference on Smart Computing (SMARTCOMP)*, 2017.

[3] Emmanuel J Candès and Benjamin Recht, "Exact matrix completion via convex optimization," *Foundations of Computational mathematics*, vol. 9, no. 6, pp. 717, 2009.

[4] E. J. Candes and T. Tao, "The power of convex relaxation: Near-optimal matrix completion," *IEEE Trans. Inf. Theory*, vol. 56, no. 5, pp. 2053–2080, 2010.

[5] R.Schimidt, "Multiple emitter location and signal parameter estimation," *IEEE Transactions on Antennas and Propagation*, vol. 34, no. 3, pp. 276–280, 1986.

[6] Y. Xu, Y. S. Shmaliy, Y. Li, and X. Chen, "Uwb-based indoor human localization with time-delayed data using efir filtering," *IEEE Access*, vol. 5, pp. 16676–16683, 2017.

[7] Lanhui Wang and Amit Singer, "Exact and stable recovery of rotations for robust synchronization," *Information and Inference: A Journal of the IMA*, vol. 2, no. 2, pp. 145–193, 2013.

[8] Rahul Mazumder, Trevor Hastie, and Robert Tibshirani, "Spectral regularization algorithms for learning large incomplete matrices," *Journal of machine learning research*, vol. 11, no. Aug, pp. 2287–2322, 2010.

[9] J.-F. Cai, E. J. Candes, and Z. Shen, "A singular value thresholding algorithm for matrix completion," *SIAM J. Optimization*, vol. 20, no. 4, pp. 1956–1982, 2010.

[10] M. Davenport and J. Romberg, "An overview of low-rank matrix recovery from incomplete observations," *IEEE Journal of Selected Topics in Signal Processing*, vol. 10, no. 4, pp. 608–622, 2016.

[11] Ward K. M. Farrell J. Lin F.-C. Karplus M. Wu, S.-M. and R. B. Smith, "Anatomy of old faithful from subsurface seismic imaging of the yellowstone upper geyser basin," *Geophysical Research Letters*, vol. 44, pp. 10240–10247, 2017.

A. MAXIMUM LIKELIHOOD ESTIMATOR

We propose another method to estimate the lag time regarding the maximal likelihood estimation. Also, we apply the model displayed in 2.1.

$$x_n(t) = s(t-\tau) + \eta_n(t), \quad t = 0, 1, 2, \cdots, T-1,$$
$$x_m(t) = s(t) + \eta_m(t), \quad t = 0, 1, 2, \cdots, T-1.$$

Suppose the noise detected by each sensor is Gaussian white noise with variance σ^2. Then the product of the two noise follows the productive normal distribution, which has a density function $K_0(\frac{|u|}{\pi\sigma^2})$, and $K_n(z)$ is a modified Bessel function of the second kind. The maximal likelihood estimation of S of each pair is

$$\hat{s}(t) = \frac{1}{2}(x_n(t+\tau) + x_m(t))$$

Also, we transfer to the frequency domain to get

$$\hat{S}(k) = \frac{1}{2}(X_n(k)e^{\tau f} + X_m(k)), \quad k = 1, 2, \cdots, T-1.$$

The Fourier Transform of a Gaussian noise follows complex Gaussian distribution, whose modulus follows Rayleigh distribution. For a fixed k, define

$$G_k(\tau) = N_n(k)^* N_m(k) = (X_n(k)\hat{S}(k)e^{-\tau f})^*(X_m(k) - \hat{S}(k)),$$

where $N_n(k) and N_m(k)$ are the Fourier Transform of Gaussian noise. $G_k(\tau)$ is the product of two Rayleigh variables. And the result comes out to be

$$\begin{aligned} N_n(k)^* N_m(k) &= (X_n(k) - \hat{S}(k)e^{-\tau f})^*(X_m(k) - \hat{S}(k)) \\ &= \frac{1}{4}(X_n(k) - X_m(k)e^{-\tau f})(X_m(k) - X_n(k)e^{\tau f}) \\ &= \frac{1}{4}(X_n(k)^* X_m(k) + X_m(k)^* X_n(k) \\ &\quad - X_n(k)^* X_n(k)e^{\tau f} - X_m(k)^* X_m(k)e^{-\tau f}) \end{aligned}$$

Suppose we get an estimation of the variance of the modulus of $N_n(k)^* N_m(k)$ to be σ_0^2, we calculate the modulus of $G_k(\tau)$, and divide it by σ_0, then it is standardized and we can approximate the distribution of $G_k(\tau)$ to be the χ^2 distribution with the degree of freedom 2. We do Monte-Carlo simulation with 20,000,000 points, and show the distribution of the product of two Rayleigh variable and a variable that follows χ^2 distribution with the degree of freedom 2 in Figure 6. The blue line represents the variable that follows the χ^2 distribution and the red line is the distribution of the product of two Rayleigh variables.

As is shown in the figure, the distribution of the product of two Rayleigh variables can be approximated by the χ^2 distribution, that is

$$\frac{|G_k(\tau)|}{\sigma_0} \sim \chi_2^2$$

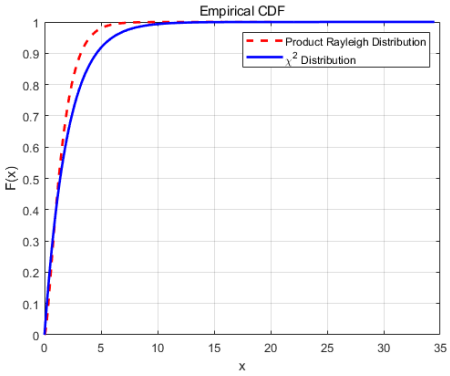

Fig. 7. Monte-Carlo simulation with 20,000,000 points

Since the samples are independent, the joint likelihood function of $G_k(0), G_k(1), G_k(2), \cdots, G_k(T-1)$ is defined to be

$$h(\tau) = \sum_{k=0}^{N-1} \log f\left(\frac{|G_k(\tau)|}{\sigma_0}\right)$$

And we should find the τ which makes h(τ) reach the max value where $f(x) = \frac{x^{-\frac{1}{2}}e^{-\frac{x}{2}}}{\sqrt{2}\gamma(\frac{1}{2})}$, which is the density function of a χ^2 variable. The estimation of τ is

$$\hat{\tau} = \arg\max_{\tau} \sum_{k=0}^{T-1} \log f\left(\frac{|G_k(\tau)|}{\sigma_0}\right)$$

Then we get a maximal likelihood estimation of the lag time. Also, if only the real or the image part of the product is considered, w.l.o.g the real part, is a sum of two productive normal variables. Then we can calculate the density function of it and find the τ maximizing the likelihood function as well.

B. REAL-DATA EXAMPLE

The cross-correlation functions between pairs of sensors, which contain signal (“peak”) and do not contain signal.

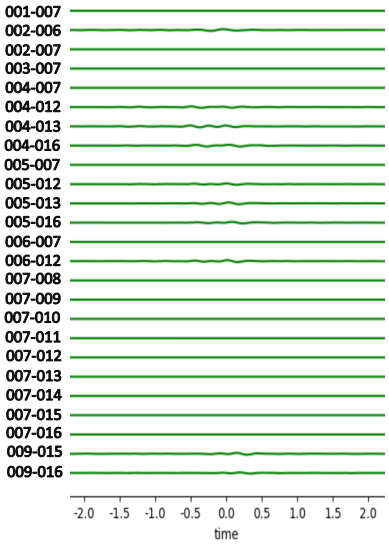

(a) No “peak”

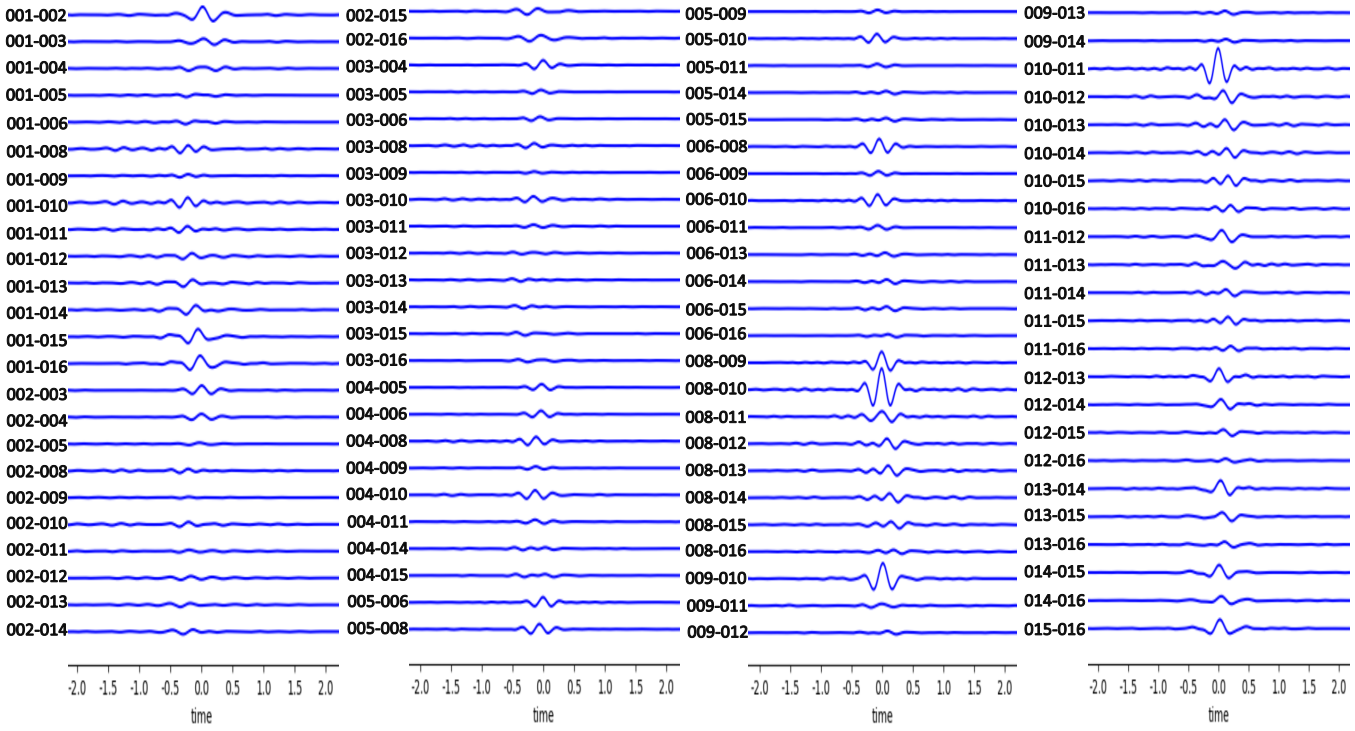

(b) Contains “peak”

Fig. 8. Results of signal detection under $\alpha = 0.1$ – cross-correlation function